MOLECULAR AND CELLULAR BIOLOGY, Nov. 2002, p. 7667–7677 Vol. 22, No. 21
0270-7306/02/$04.00+0 DOI: 10.1128/MCB.22.21.7667–7677.2002

Defective Associations between Blood Vessels and Brain Parenchyma Lead to Cerebral Hemorrhage in Mice Lacking αv Integrins

Joseph H. McCarty,[1] Rita A. Monahan-Earley,[2] Lawrence F. Brown,[2] Markus Keller,[3] Holger Gerhardt,[4] Kristofer Rubin,[5] Moshe Shani,[6] Harold F. Dvorak,[2] Hartwig Wolburg,[4] Bernhard L. Bader,[3] Ann M. Dvorak,[2] and Richard O. Hynes[1]*

Howard Hughes Medical Institute and Center for Cancer Research, Massachusetts Institute of Technology, Cambridge, Massachusetts 02139[1]; Department of Pathology, Beth Israel-Deaconess Medical Center, and Harvard Medical School, Boston, Massachusetts 02215[2]; Department of Protein Chemistry, Max Planck Institute for Biochemistry, Martinsried, Munich, Germany[3]; Institute of Pathology, University of Tübingen, Tübingen, Germany[4]; Department of Medical and Physiological Chemistry, University of Uppsala, Uppsala, Sweden[5]; and Institute for Animal Science, The Volcani Institute, Bet Dagan, Israel[6]

Received 17 June 2002/Accepted 1 August 2002

Mouse embryos genetically null for the αv integrin subunit develop intracerebral hemorrhages at midgestation and die shortly after birth. A key question is whether the hemorrhage arises from primary defects in vascular endothelial cells or pericytes or from other causes. We have previously reported normal initiation of cerebral vessels comprising branched tubes of endothelial cells. Here we show that the onset of hemorrhage is not due to defects in pericyte recruitment. Additionally, most αv-null vessels display ultrastructurally normal endothelium-pericyte associations and normal interendothelial cell junctions. Thus, endothelial cells and pericytes appear to establish their normal relationships in cerebral microvessels. However, by both light and electron microscopy, we detected defective associations between cerebral microvessels and the surrounding brain parenchyma, composed of neuroepithelial cells, glia, and neuronal precursors. These data suggest a novel role for αv integrins in the association between cerebral microvessels and central nervous system parenchymal cells.

Vascularization of the developing vertebrate brain occurs exclusively via angiogenesis, i.e., the formation of new blood vessels from existing vasculature (26). Capillaries originating in the perineural vascular plexus begin to invade the mouse neuroectoderm as early as embryonic day 10.0 (E10.0). Even at the early stages of cerebral angiogenesis, the microvessels become associated with perivascular mural cells, i.e., pericytes. Once within the neuroectoderm, vascular endothelial cells come in close contact with other brain parenchymal cell types, including neuroblasts, neuroepithelial cells, radial glia, and astrocytes (5, 25, 30). These multicellular interactions eventually form the highly selective barrier between blood and brain (4, 33, 34).

While several factors necessary for proper endothelial cell-pericyte interactions have been identified and characterized (18, 20, 21, 36), very little is known about the molecular interactions between blood vessels and cells of the brain parenchyma. Recent data, however, support important roles for cell-extracellular matrix adhesion events involving members of the αv integrin family of cell surface receptors (27).

We previously generated a mouse strain genetically null for all five members of the αv integrin subfamily (3). αv gene ablation causes 100% lethality; however, overall development, including vasculogenesis and angiogenesis, proceeds normally until E9.5. Between E10.5 and E11.5 approximately 70% of the αv-null embryos die, probably because of placental defects (3). By E12.5, the surviving αv-null embryos develop vascular defects typified by cerebral blood vessel dilation and hemorrhage. The hemorrhage initially forms within the ganglionic eminences of the developing telencephalon and subsequently spreads throughout the brain. αv-null neonates are severely hydrocephalic and die within hours after birth.

In this study we characterized the cellular events responsible for the cerebral hemorrhage found in αv-null embryos. The origins of these defects could lie in the endothelial cells, in the microvascular pericytes, or in the interactions between them or with the surrounding neural cells. Light and electron microscopic analyses revealed normal recruitment and association of pericytes with endothelial cells in the cerebral microvessels. However, we detected defective ultrastructural interactions between cerebral microvessels and surrounding central nervous system parenchymal cells. Collectively, these data support a novel role for αv integrins specifically in the establishment and maintenance of vascular integrity via interactions between cerebral microvessels and central nervous system parenchymal cells.

MATERIALS AND METHODS

Mouse husbandry and PCR genotyping. Heterozygous mice (129SvJae/C57BL6/FVB mixed genetic background) were interbred to generate αv-null embryos. Noon of the plug date was defined as E0.5. The transgenic mouse strain expressing *lacZ* in vascular smooth muscle cells (vSMC)/pericytes has been described in detail elsewhere (37). $lacZ^+$ males (FVB) were crossed to $\alpha v^{+/-}$ females (C56BL6/129SvJae), and blastocysts were transferred to recipient mothers. The resulting rederived $\alpha v^{+/-}$ $lacZ^+$ progeny were interbred, and αv-null/$lacZ^+$ embryos were identified by PCR genotyping of the yolk sac (3, 37). When

* Corresponding author. Mailing address: M.I.T. E17-230, Cambridge, MA 02139. Phone: (617) 253-6422. Fax: (617) 253-8357. E-mail: rohynes@mit.edu.

necessary, E10.5 class I and II αv-nulls were distinguished based on overall embryo size and obvious placental layering defects (3). To generate mice deficient for both β3 and β5 integrins (22, 23), null strains were interbred, and subsequent double-homozygous nulls were mated to generate embryos.

Antibodies. The rabbit anti-NG2 polyclonal antiserum (Chemicon International Inc., Temecula, Calif.) and the anti-PECAM-1/CD31 rat monoclonal antibody (platelet endothelial cell adhesion molecule [PECAM]; Pharmingen, San Diego, Calif.) were both used at 1:200 dilutions. The anti-platelet-derived growth factor receptor beta rabbit polyclonal antibody sc-432 (Santa Cruz Biotech, Santa Cruz, Calif.) was used at a concentration of 7.5 μg/ml. The rabbit antifibronectin antiserum (32) was used at a 1:250 dilution. Antinestin (Rat-401) and anti-RC2 hybridoma supernatants were purchased from the Developmental Studies Hybridoma Bank (Iowa City, Iowa) and used at 1:3 and 1:2 dilutions, respectively. The swine anti-rabbit immunoglobulin secondary antibody used for chromogenic analysis was purchased from Dako (Carpenteria, Calif.). Secondary antibodies for immunofluorescence were Alexa-conjugated goat anti-rabbit immunoglobulin G (IgG), goat anti-mouse IgG and IgM, and goat anti-rat IgG; all were purchased from Molecular Probes (Eugene, Oreg.).

Immunohistochemistry. Embryos from various developmental stages were decapitated, and the heads were fixed in ice-cold 4% paraformaldehyde for 4 h. Heads were infiltrated in 30% sucrose–phosphate-buffered saline overnight at 4°C and embedded in Tissue Tek OCT (Miles, Elkhart, Ind.). Coronal sections were blocked with 2% fish oil–4% mouse serum–4% swine serum in phosphate-buffered saline. Chromogenic visualization procedures were performed according to the Vectastain ABC kit protocol (Vector Laboratories, Burlingame, Calif.), with the exception that swine anti-rabbit immunoglobulin secondary antibody was used in place of the secondary antibody provided by the manufacturer. For immunofluorescence staining, Alexa-conjugated secondary antibodies were used at 1:500 dilutions.

Light and electron microscopy. Semithin sections were prepared by fixing embryonic heads in cold 10% formalin overnight. The tissue was washed extensively and processed according to the manufacturer's instructions (Polysciences, Inc., Warrington, Pa.). Sections (1 μm) were prepared, and the tissue was visualized with a methyl green counterstain. Paraffin-embedded sections were counterstained with hematoxylin and eosin. All images were visualized with a Zeiss Axiophot photoscope. Images were processed with NIH Scion Image and Adobe Photoshop (Adobe, Mountain View, Calif.). For confocal microscopy, coronal thick sections (35 μm) from OCT-embedded E11.5 and E12.5 heads were analyzed with a Zeiss LSM 510 confocal microscope (Carl Zeiss, Oberkochen, Germany). Anti-NG2 and anti-CD31/PECAM antibodies were used to identify pericytes and endothelial cells, respectively. To quantitate pericyte coverage, 25-μm z-series were scanned at 3-μm intervals. Pericyte cell bodies (as defined by NG2 positivity) were quantitated along individual PECAM/CD31-positive vessels. Processing and analysis of E11.5 (data not shown) and E12.5 samples for electron microscopy were performed as previously described (13).

RNase protection assays. Primers were designed and standard PCR-based methods were used to amplify cDNA sequences for mouse vascular endothelial growth factor A (nucleotides 97 to 529), PECAM (nucleotides 113 to 1051), Hif1α (nucleotides 2869 to 3773), Flk-1 (nucleotides 4339 to 5294), and smooth muscle α-actin (nucleotides 77 to 978). The various cDNAs were subcloned into the pTopoII vector (InvitroGen), and the T7 or SP6 RNA polymerase promoter was used to generate RNA templates. The sizes of the protected fragments were as follows: Flk-1, 646 bp; smooth muscle α-actin, 349 bp; Hif1α, 175 bp; PECAM, 462 bp; vascular endothelial growth factor A, 450 bp; and human β-actin, 127 bp (purchased from Ambion). Embryos from developmental ages E11.5 to E13.5 were dissected, and telencephalic and diencephalic regions were isolated. Total RNA was purified with the RNeasy extraction kit (Qiagen, Valencia, Calif.). Ten micrograms of total RNA was used with the various RNA probes.

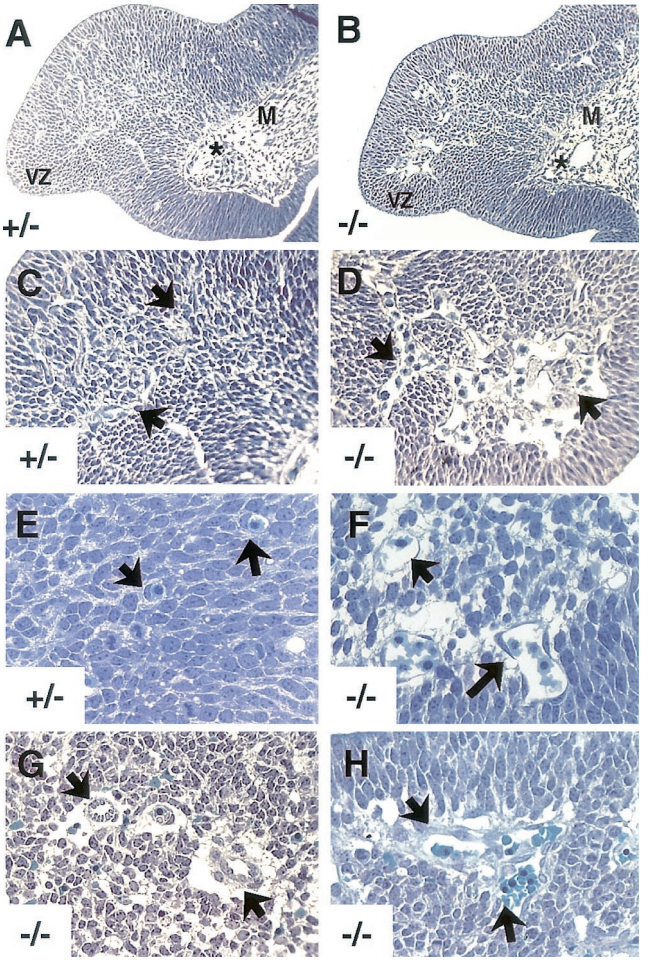

FIG. 1. Transverse sections through E10.5, E11.5, and E12.5 ganglionic eminences. (A to D) Expanded lumenal areas in E10.5 αv-null cerebral vessels. In both the $\alpha v^{+/-}$ (A) and $\alpha v^{-/-}$ (B) brains, perineural vascular plexus vessels (asterisks in A and B) align along the leptomeningeal boundary and migrate into the brain parenchyma. Unlike the heterozygous controls (A and C), $\alpha v^{-/-}$ embryos displayed abnormally large vessel lumens as they neared the ventricular zone (arrows in D). (E and F) αv-null cerebral vessels contain thinned areas of endothelial cell cytoplasm and do not adhere closely to the surrounding neural tissue. E11.5 $\alpha v^{+/-}$ vessels (arrows in E) are closely juxtaposed with surrounding neural cell types. $\alpha v^{-/-}$ ganglionic eminence vessels contained slightly thinned regions of endothelial cell cytoplasm and the first signs of space forming between the microvessels and the adjacent neural tissue (arrows in F). (G and H) Hemorrhage in E12.5 $\alpha v^{-/-}$ brains. $\alpha v^{-/-}$ vessels were structurally disorganized and contained endothelial cell entanglements (arrows in H). Note the abnormally high number of endothelial cell nuclei protruding into the vessel lumens (arrows in G). Abbreviations: M, meningeal compartment; VZ, ventricular zone.

RESULTS

Light microscopic analysis of αv-null cerebral hemorrhage. Vascularization of the central nervous system begins at ≈E10.0 of mouse development, when angiogenic vessels from the perineural vascular plexus invade the embryonic neuroectoderm (26, 33). At E10.5 in both $\alpha v^{-/-}$ and $\alpha v^{+/-}$ brains, we detected normal alignment and invasion of vessels from the perineural vascular plexus into the developing ganglionic eminences (Fig. 1A and B). In αv-null brains (Fig. 1B and D), vessels nearing the ganglionic eminence ventricular zone displayed abnormally large lumens. However, the lining endothelium was intact, and there were no grossly obvious signs of edema or hemorrhage. Similar lumenal expansions were also observed elsewhere in the brain parenchyma (data not shown).

By E11.5, the vessels in the αv-null ganglionic eminences showed initial signs of distension and endothelial cytoplasmic thinning (Fig. 1F). Also notable were significant spaces between the mutant blood vessels and the surrounding neural

tissue (Fig. 1F). This contrasted with the nondistended endothelium and close juxtaposition between vessels and adjacent cells normally found in sections from the heterozygous control brains (Fig. 1E). At E12.5, vessels in the αv-null ganglionic eminences were distended and generally disorganized and exhibited extensive hemorrhage (Fig. 1G and H). E12.5 αv-null sections also showed increased spaces between the surrounding brain tissue and the blood vessels (Fig. 1G and H).

One possible explanation for the observed hemorrhage was that hypoxia-induced regulation of the vascular endothelial growth factor (VEGF) signaling pathway might be perturbed in the αv-null embryos. To address this possibility, RNase protection assays were used to analyze the brain-specific expression of transcripts encoding VEGF and its endothelial cell-specific receptor, Flk. When analyzed at E11.5, a time of altered vascular morphology yet prior to the onset of hemorrhage, we detected normal expression levels of VEGF and Flk transcripts (Fig. 2). Thus, upregulation of VEGF signaling components does not precede the abnormal cerebral microvessel characteristics in the αv-null embryos.

At E13.5, a time when extensive hemorrhage had begun, a marked increase in Flk and VEGF-A mRNA was detected in αv-null brains. The upregulation of the Flk transcript correlated with increased expression of both the endothelium-specific PECAM/CD31 and the pericyte-specific smooth muscle α-actin gene products. These data collectively suggest that, subsequent to the onset of cerebral hemorrhage, vascular cell hyperproliferation may be occurring in the αv-null brain. It should be noted that the increased expression of the various mRNAs was localized mainly to the developing diencephalon and telencephalon. RNase protection assays performed with total RNA isolated from whole embryo heads did not yield detectable increases for any of the transcripts tested. Lastly, the localized increases also matched in situ hybridization analyses with RNA probes specific for VEGF and Flk (data not shown).

Immunohistochemical analysis of pericyte coverage in αv-null brains. Pericytes are vascular mural cells that associate intimately with the microvascular endothelium and influence vessel function (reviewed in reference 6). We addressed whether the microvascular hemorrhage observed in the αv-null embryos was associated with defects in the recruitment of pericytes, as has been described for other strains of mutant mice (21). E11.5 brain sections were analyzed for microvascular pericytes with anti-platelet-derived growth factor receptor beta (Fig. 3A and B) and anti-NG2 antibodies (Fig. 3C and D) (20, 31). As shown in Fig. 3A to D, in the absence of αv integrins, pericytes were associated with all the cerebral microvessels. We did not observe cerebral microvessels lacking pericyte coverage. Similarly, 5-bromo-4-chloro-3-indolyl-β-D-galactopyranoside (X-Gal) staining of tissue sections from E11.5 αv-null brains expressing a pericyte-specific *lacZ* transgene also demonstrated blood vessel coverage by pericytes (Fig. 3E and F).

To determine any quantitative differences in pericyte coverage, confocal laser scanning microscopy was used to assess pericyte numbers. Anti-PECAM-1/CD31 antibody was used to identify endothelial cells, and anti-NG2 was used to visualize pericytes (Fig. 4A and B). All PECAM-positive structures had associated pericytes. One hundred vessels from E11.5 heads

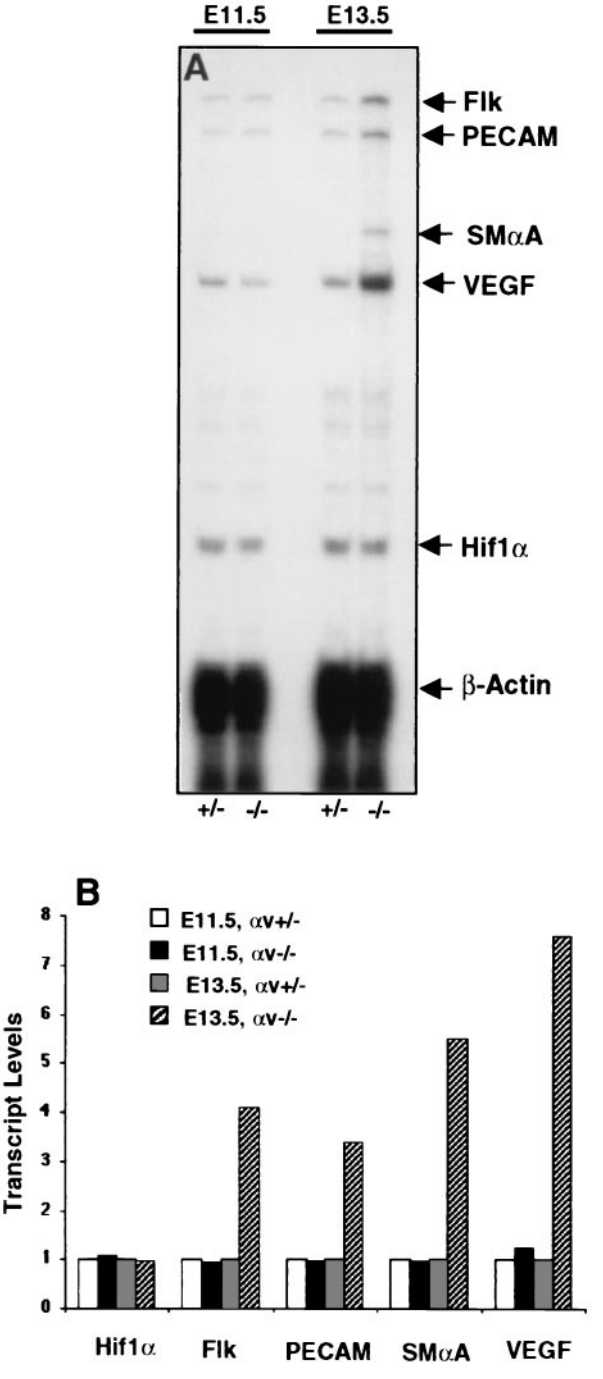

FIG. 2. RNase protection assays with RNA isolated from E11.5 and E13.5 telencephalon and diencephalon. Total RNA isolated from E11.5 and E13.5 brain regions was used to determine the relative mRNA levels for VEGF, Flk, PECAM, smooth muscle α-actin (SMαA), and Hif1α. Shown is one representative experiment of three. Note the marked upregulation of expression of VEGF, Flk, PECAM, and smooth muscle α-actin only in hemorrhagic E13.5 $αv^{-/-}$ embryo brains. No changes in any transcript levels were present at E11.5, a developmental time point showing vascular abnormalities but no hemorrhage.

were analyzed by counting the number of NG2-positive pericyte cell bodies along a 25-μm traverse. No quantitative difference in pericyte-endothelial cell coverage was observed between αv-null and heterozygous brains (Fig. 4C). Comparisons

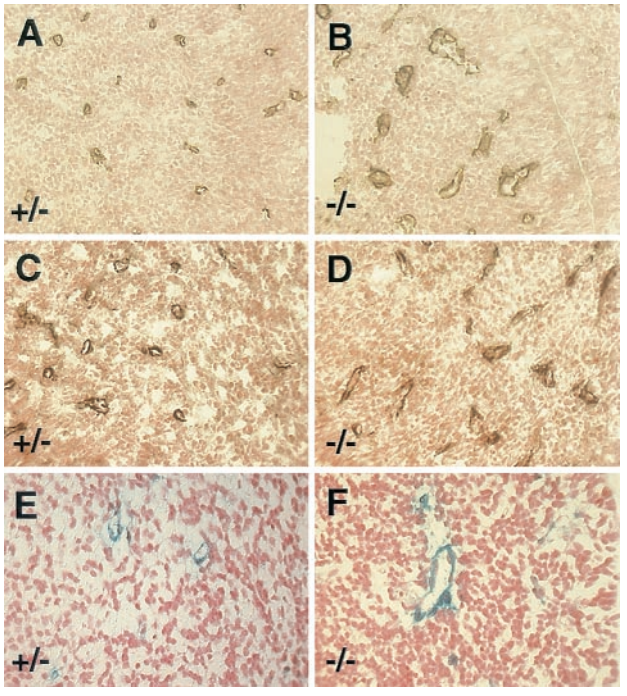

FIG. 3. Pericytes are recruited normally to $\alpha v^{-/-}$ cerebral vessels. Frozen sections from E11.5 $\alpha v^{+/-}$ (A, C, and E) and $\alpha v^{-/-}$ (B, D, and F) embryonic heads were immunolabeled with anti-NG2 (A and B) or anti-platelet-derived growth factor receptor beta (C and D) antibodies. Paraffin sections from αv-heterozygous or homozygous null embryos expressing *lacZ* in pericytes were stained with X-Gal (E and F). All three pericyte markers are normally associated with $\alpha v^{-/-}$ vessels.

at E12.5 were difficult because $\alpha v^{-/-}$ vessels were distended and disorganized (Fig. 4D) and very few vessels were similar in size to those found in $\alpha v^{+/-}$ control brain sections.

Electron microscopic analysis of αv-null brains. Ultrastructural analysis of $\alpha v^{+/+}$ and $\alpha v^{+/-}$ cerebral microvessels and their surrounding pericytes at E12.5 revealed generally nondilated vessels and normally associated endothelial cells and pericytes. Endothelial cells enclosed luminal spaces that contained nucleated red blood cells (Fig. 5A). Endothelial cells were connected by mature cell junctions with elongated endothelial cell flaps on their luminal surfaces (Fig. 5A). Basal laminae were poorly developed in E12.5 microvessels compared with newborn mouse brain microvessels (H. Wolburg, B. L. Bader, S. Stiver, D. Feng, and A. M., Dvorak, unpublished data). Discontinuous foci of basal lamina beneath abluminal endothelial cell surfaces were also noted.

All $\alpha v^{+/+}$ and $\alpha v^{+/-}$ microvessels were invested with pericytes. Pericytes were eccentrically located, and when sections traversed their nuclei, one could follow narrow cytoplasmic processes extending for long distances immediately adjacent to endothelial cells (Fig. 5A). $\alpha v^{+/+}$ and $\alpha v^{+/-}$ E12.5 embryonic pericytes were not completely mature in that their normal investiture with basal lamina was poorly developed and their cytoplasm was virtually devoid of microfilaments and surface-connected caveolae (Fig. 5A). Thus, at the embryonic ages studied, pericytes, although present, had not assumed a mature, contractile phenotype.

In contrast, E12.5 $\alpha v^{-/-}$ cerebral microvessels (Fig. 6) dis-

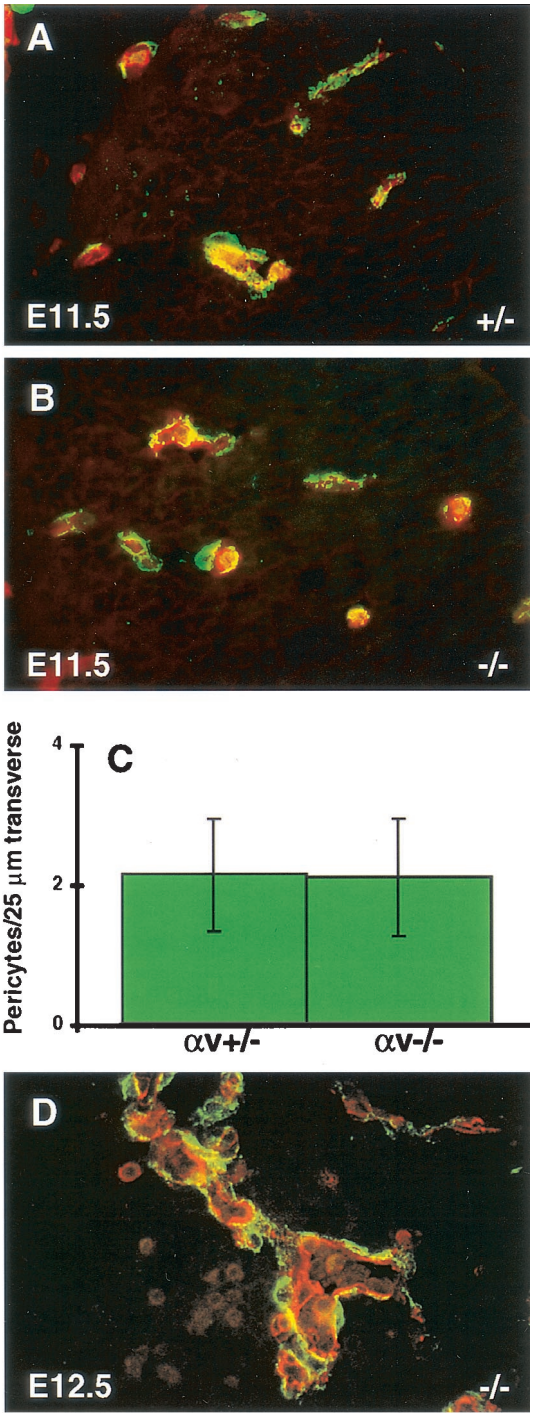

FIG. 4. Immunofluorescence analyses of cerebral microvessels and quantitation of pericyte association. Frozen sections from $\alpha v^{+/-}$ (A) or $\alpha v^{-/-}$ (B and D) embryonic heads were fluorescently labeled with anti-PECAM (red) and anti-NG2 (green) antibodies. Within $\alpha v^{+/-}$ and $\alpha v^{-/-}$ sections, cerebral microvessels of similar sizes were selected for quantitation by confocal microscopy. The number of NG2-positive pericyte cell bodies along individual E11.5 vessels (PECAM positive) per 25 μm of transverse section was counted for 100 vessels. No quantitative comparison between E12.5 $\alpha v^{+/-}$ and $\alpha v^{-/-}$ samples was possible due to the extreme distension of the αv-null vessels (D).

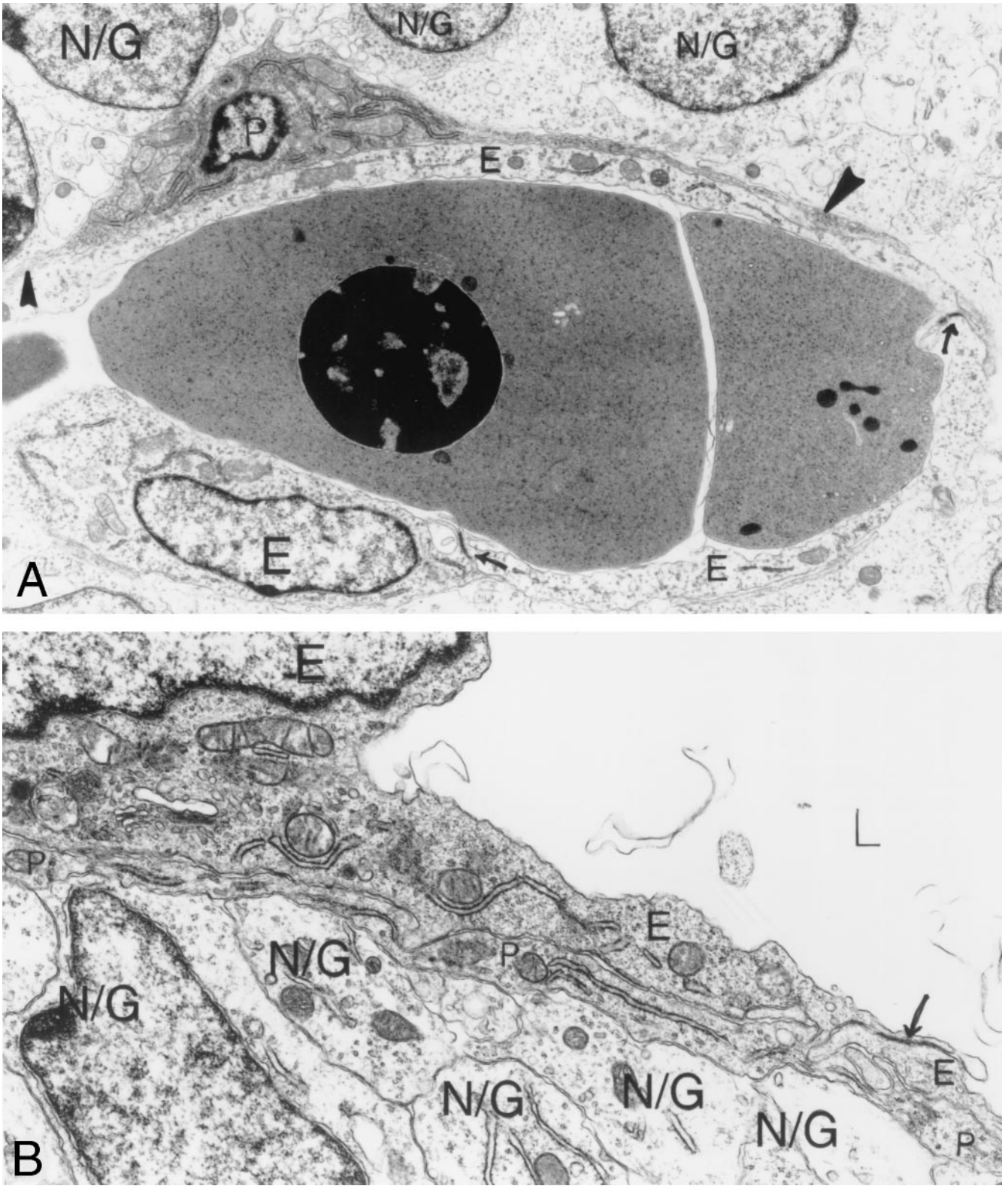

FIG. 5. Ultrastructural analysis of E12.5 $\alpha v^{+/-}$ cerebral microvessels. (A) Vascular lumen seen in longitudinal section, containing nucleated red blood cells. Normal endothelial cells (E) with closed junctions (arrows) line the lumen. One pericyte (P) has two long, narrow processes in view (solid arrowheads). Overlying brain parenchymal cells are in contact with the pericyte beneath. (B) Another view of an $\alpha v^{+/-}$ cerebral microvessel shows an empty vascular lumen, two normal endothelial cells (E) connected by a closed interendothelial junction (arrow). A pericyte process (P) covers the two endothelial cells. Brain parenchymal cells and their processes (N/G) cover the overlying pericyte process completely, with little to no intervening space. Magnification: (A) 8,000×; (B) 15,500×. Abbreviations: E, endothelial cells; P, pericytes; N/G, brain parenchymal cells.

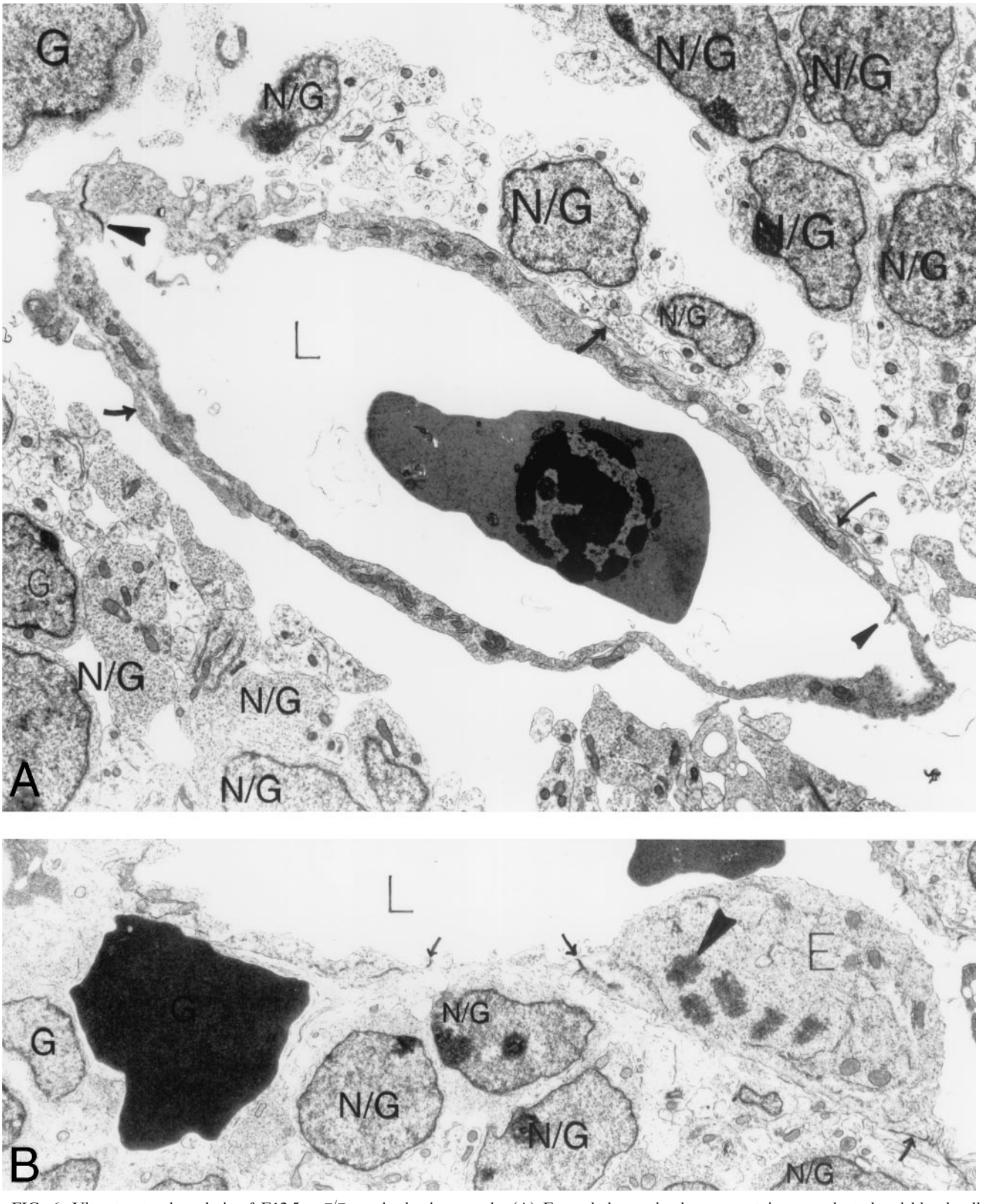

FIG. 6. Ultrastructural analysis of E12.5 $\alpha v^{-/-}$ cerebral microvessels. (A) Expanded vascular lumen contains a nucleated red blood cell; endothelial cells line the lumen and are closed by normal interendothelial cell junctions (solid arrowheads). Although pericyte cell bodies were absent in this section, pericyte processes in contact with the endothelium were seen (arrows). Numerous round brain parenchymal cells (N/G) and their foot processes are visible in the perivascular sheath. Some of the foot processes contact a pericyte process; very few contact endothelial cells. There is an extensive space surrounding the entire vessel. (B) Extravasated red blood cell rests among brain parenchymal cells (N/G) beneath the endothelium with closed interendothelial cell junctions (arrows). An enlarged endothelial cell (E) is protruding into the vascular lumen (L) and undergoing mitosis (solid arrowhead marks a chromosome). Magnification: (A) 6,000×; (B) 13,000×. Abbreviations: E, endothelial cells; N/G, brain parenchymal cells.

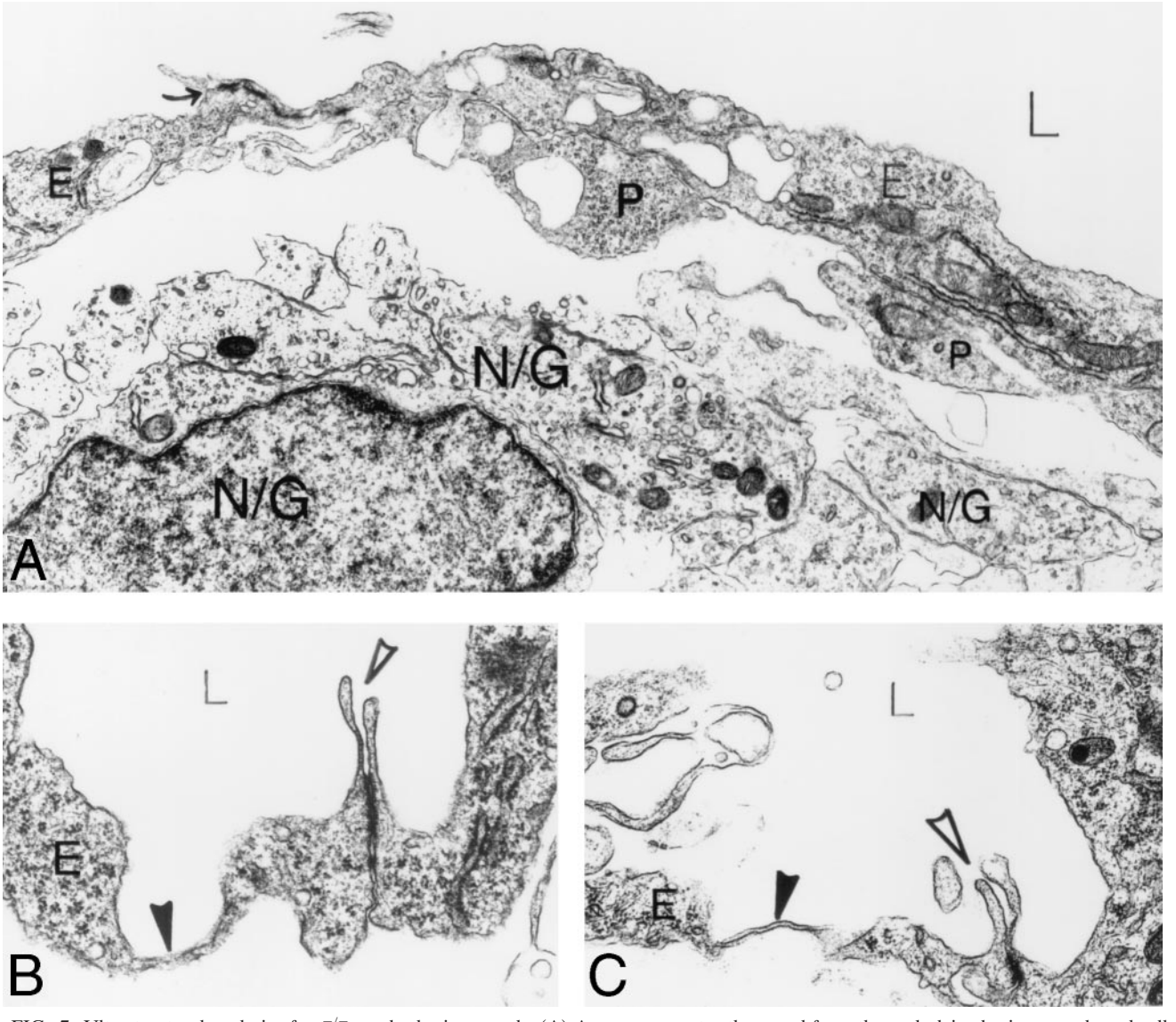

FIG. 7. Ultrastructural analysis of $\alpha v^{-/-}$ cerebral microvessels. (A) A space separates the vessel from the underlying brain parenchymal cells (N/G). Several pericyte processes (P) contact endothelial cells (E), which line the lumen (L) of the vessel. Large membrane-bound vacuoles are seen within endothelial cells and pericytes. An interendothelial cell junction is closed (arrow). Panels B and C show focal (B) and flat (C) parajunctional thinned endothelial cell cytoplasm (solid arrowheads). Note that the interendothelial cell junctions (open arrowheads) are normal, guarded by endothelial cell flaps, and are tightly closed. Magnification: (A) 10,000×; (B and C) 24,000×. Abbreviations: E, endothelial cells; P, pericytes; N/G, brain parenchymal cells.

played extensive luminal expansion and tortuosity (Fig. 6A) and marked focal thinning of endothelial cytoplasm (Fig. 7B and C). Focal increases in large cytoplasmic vacuoles in both endothelial cells and pericytes were noted (Fig. 7A). Mature, well-formed endothelial cell junctions were present; none of these showed gap formation or discontinuities (Fig. 6 and 7). Nucleated red blood cells were present within vessel lumina and were also found adjacent to microvessels in the loosened perivascular sheaths (Fig. 6B). Pericytes were present in αv-null samples and displayed normally extended narrow processes in close association with underlying endothelium (Fig. 6A and 7A). However, some enlarged, tortuous vessels with expanded extravascular spaces were not as well invested with pericyte processes.

The perivascular sheath in $\alpha v^{+/+}$ and $\alpha v^{+/-}$ embryos was composed of an imperfect but close investiture by brain parenchymal cells (Fig. 5). Brain parenchymal cells were large and filled primarily with free ribosomes; they had numerous wide, elongated blunt surface processes that extended to and often lined the abluminal surface of underlying pericytes (Fig. 5A and 5B) or occasionally directly abutted abluminal surfaces of endothelial cells in areas devoid of pericytes (data not shown). These parenchymal cell extensions are referred to as endfeet. They were relatively organelle free, with an electron-lucent appearance, which allowed easy distinction from more electron-dense pericyte processes (Fig. 5A and 5B).

The most striking finding in the E12.5 αv-null embryonic cerebral microvessels was the presence of extensive spaces

separating the parenchymal cells from the microvessels and their pericyte sheaths (Fig. 6 and 7). The majority of αv-null vessels showed significant separation between the vascular cells (endothelial cells and pericytes) and the surrounding brain parenchyma. When process formation and parenchymal endfeet were visible, they contacted bare endothelium and, less frequently, pericyte cell processes (Fig. 6A and 7A). However, parenchymal cells were most often widely separated from the perivascular-pericyte sheath, were often rounded with minimal evidence of processes and endfeet, and, when these were visible, they often did not contact pericytes or endothelial cells (Fig. 6A and 7A).

Abnormal neuroglial process elaboration in αv-null brains. Based on the ultrastructural observations, we did further studies to classify the brain parenchymal cells associated with cerebral microvessels. The antinestin monoclonal antibody Rat-401 was used to visualize the neuroepithelial and neuronal precursor cells. Cerebral blood vessels were identified with a polyclonal antiserum recognizing fibronectin, a primary component of the vascular basement membrane. As shown in Fig. 8A, E12.5 $\alpha v^{+/+}$ control sections showed neuroepithelial cells apparently spanning the developing ganglionic eminence. In contrast, E12.5 αv-null neuroepithelial processes did not seem to extend normally through the ganglionic eminences (Fig. 8B and C). αv-null neuroepithelial processes within the ganglionic eminences made contacts with cerebral vessels, yet they appeared disordered and were generally less elaborate. A distinct punctate antinestin immunoreactive pattern was present surrounding many microvessels in $\alpha v^{-/-}$ ganglionic eminences (Fig. 8C). E11.5 αv-null sections showed a similar nestin immunoreactivity surrounding cerebral microvessels (data not shown). Likewise, a similar punctate immunoreactive pattern was observed at E11.5 and E12.5 with the RC2 monoclonal antibody, which recognizes an epitope specific to central nervous system neuroepithelial cells (data not shown).

Cerebral hemorrhage is not caused by loss of αvβ3 and αvβ5 integrins. The αv-null mutation eliminates all five αv integrins. Only two of these, αvβ3 and αvβ5, have been detected on endothelial cells. To address whether loss of the αvβ3 and αvβ5 integrins was involved in the cerebral hemorrhage formation, we interbred mice singly null for the β3 and β5 genes (22, 23). β3/β5-deficient animals were viable and fertile. Embryos null for both integrin subunits were dissected and analyzed. E12.5 β3/β5-null embryos studied from several litters displayed no gross or microscopically detectable cerebral hemorrhages (Fig. 9 and data not shown).

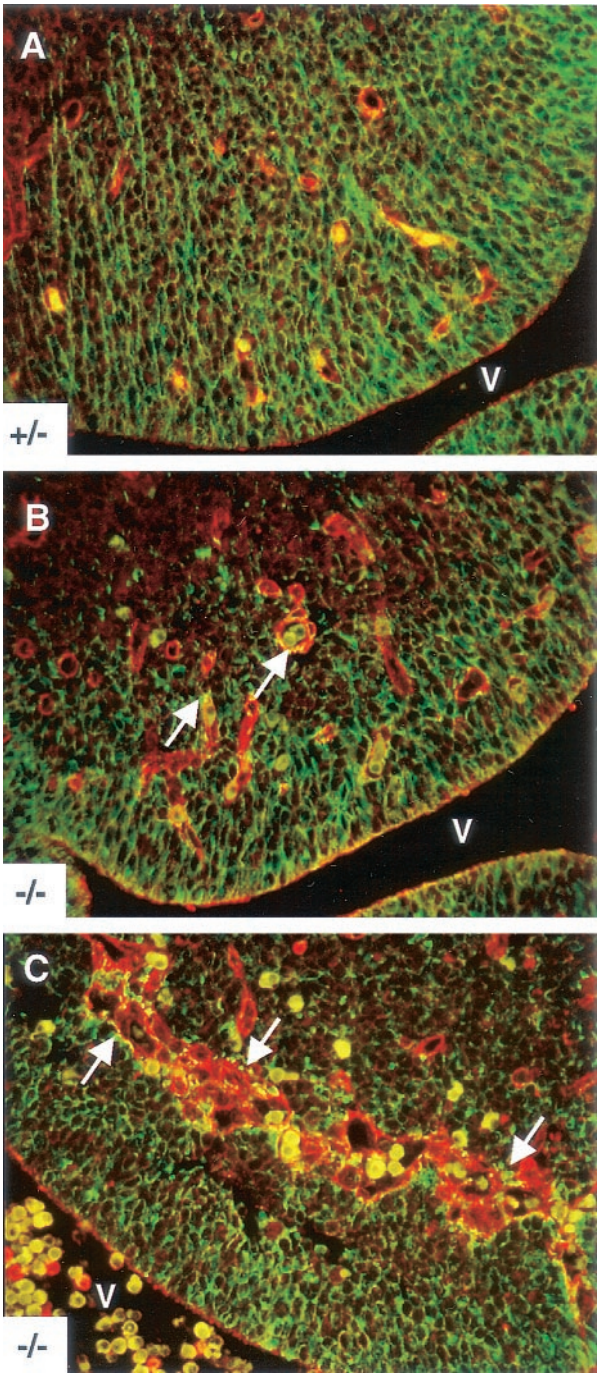

FIG. 8. Disorganized neuroepithelial processes in αv-null ganglionic eminences. E12.5 paraffin-embedded transverse sections from αv-heterozygous control (A) or αv-null (B and C) brains were immunolabeled with antinestin monoclonal antibody to visualize the neuroepithelial cells (green). Antifibronectin antiserum was used to label the cerebral microvessels (red). Erythrocytes appear yellow. Elaborate neuroepithelial processes span the ganglionic eminence and make contact points with vessels in the $\alpha v^{+/-}$ control section (A). In an αv-null ganglionic eminence region (B) devoid of significant vessel distension or hemorrhage, note the less elaborate neuroepithelial cell organization. A punctate nestin immunoreactivity is seen associated with many $\alpha v^{-/-}$ microvessels (arrows in B). Disorganized neuroepithelial processes and nestin-immunoreactive puncta (arrows in C) are more obvious in a ganglionic eminence region containing pronounced microvessel distension and hemorrhage. Abbreviations: V, ventricle.

DISCUSSION

A primary goal of this study was to identify the primary cellular defects contributing to cerebral hemorrhage in αv-null mice. The integrins αvβ3 and αvβ5 are expressed on angiogenic endothelial cells, and an extensive body of literature suggests important roles for these integrins during developmental and pathological angiogenesis (7, 8, 12, 16, 17). However, apart from the localized cerebral hemorrhage, developmental vasculogenesis and angiogenesis occur normally in the absence of all αv-containing integrins (3). If αv gene deletion resulted in general endothelial cell defects, one would expect to see widespread vascular abnormalities. Indeed, genetic ab-

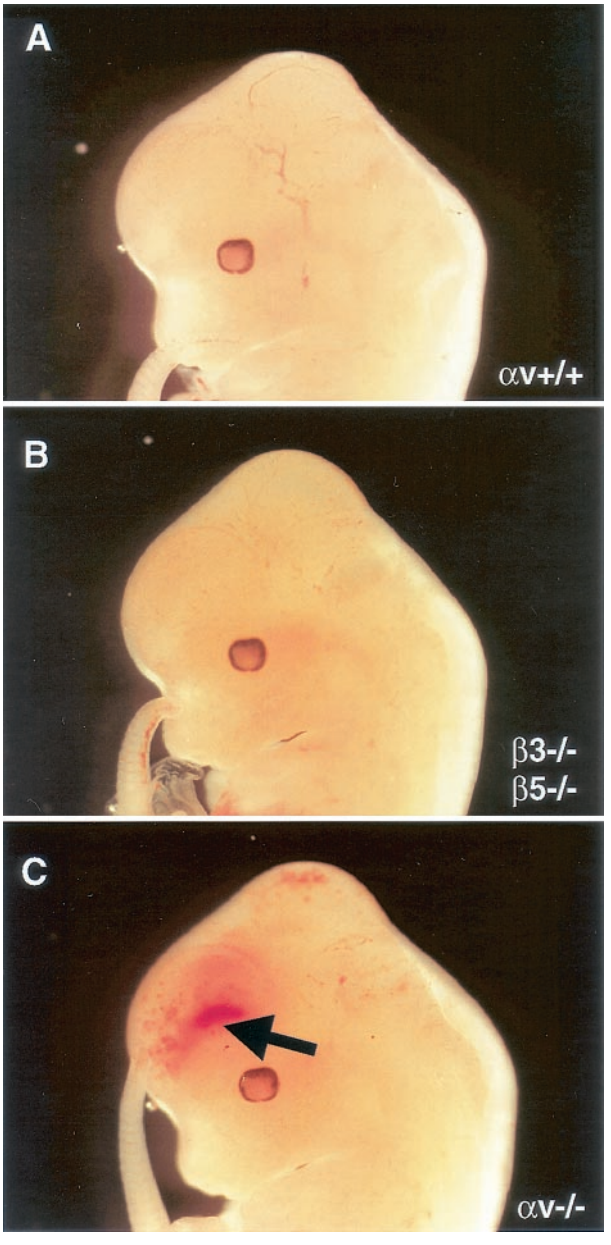

FIG. 9. Absence of αvβ3 and αvβ5 does not lead to cerebral hemorrhage. E12.5 embryos, either wild type (A), null for both β3 and β5 integrin genes (B), or null for all five αv integrins (C), were dissected and analyzed. Only embryos lacking all αv integrins displayed grossly visible cerebral hemorrhage (arrow in C).

lation of endothelium-specific factors such as VEGF-A and VE-cadherin leads to profound embryonic vascular phenotypes (9, 10, 15). Therefore, it is unlikely that primary endothelial cell defects contribute to the observed vascular phenotype. Furthermore, embryos null for both the β3 and β5 genes (and therefore lacking the αvβ3 and αvβ5 integrins) do not develop cerebral hemorrhage (Fig. 9).

One could argue that the abnormal vessel characteristics and cerebral hemorrhage are a secondary consequence of hypoxic conditions in the developing embryonic brain. Indeed, hemorrhagic E13.5 αv-null brains do show upregulation of the hypoxia-inducible genes for Flk and VEGF (Fig. 2). However, our light microscopic analyses revealed microvessel expansion at E10.5 and compromised vascular integrity as early as E11.5, prior to any measurable increases in the VEGF or Flk transcripts. Thus, increased expression of the VEGF and Flk transcripts appears to be a result rather than a cause of the cerebral hemorrhage.

A pericyte recruitment defect was also considered as a primary cause for the αv-null hemorrhage. Multiple signaling pathways are necessary for the proper establishment of endothelial cell-pericyte associations. and in many cases, disruption of these signaling events leads to defective pericyte recruitment and microvascular hemorrhage (18, 21). However, we did not detect pericyte recruitment defects in αv-null brains (Fig. 3). Moreover, quantitation of pericyte number revealed no significant difference between control and αv-null brains (Fig. 4). Transmission electron microscopic analysis of $\alpha v^{-/-}$ embryos revealed some expanded endothelial regions that were poorly covered or not covered at all by pericyte processes. However, most αv-null microvessels displayed relatively normal cell contact between cytologically normal endothelial cells and pericytes (Fig. 6 and 7). Thus, the vascular defects observed in the αv-null embryos do not appear to correlate directly with a primary pericyte abnormality.

Interestingly, the extreme vessel pathology present within the αv-null brain parenchyma was not observed in the perineural vascular plexus (data not shown). Here, vessel dilation and hemorrhage were rare, pointing to the selectivity of the defect for vessels within the brain microenvironment. Consistent with this idea, our electron microscopic analyses revealed ultrastructural defects in the associations between the vessels (endothelial cells plus pericytes) and surrounding brain parenchymal cells (Fig. 6 and 7).

Beginning at ≈E10.5, during vertebrate embryogenesis, newly differentiated neurons migrate from ventricular zones towards the pial surface of the brain along glial cell processes (1, 11). Interestingly, αv integrin immunolocalizes to radial glial cell processes in cultured E14.5 embryonic cortical slices (2). While we have yet to conclusively immunolocalize αv on glial cell processes at E11.5 or E12.5, our immunohistochemical analyses show a disorganized neuroepithelium in E11.5 (data not shown) and E12.5 αv-null brain sections (Fig. 7). A distinct punctate pattern of nestin immunoreactivity is associated with many αv-null vessels. These puncta appear to represent fragmented neuroepithelial processes; these may conform to similar structures observed by electron microscopic analysis in the αv-null brain parenchyma (Fig. 6 and 7).

The αv subunit can associate with five distinct beta subunits, yielding integrins αvβ1, αvβ3, αvβ5, αvβ6, and αvβ8. Deletion of the β1 gene leads to early embryonic lethality (14), prior to the onset of cerebral hemorrhage observed in the αv-nulls. However, mice harboring a conditional deletion of the β1 subunit in neuronal precursors and central nervous system glia develop to term and do not develop gross cerebral hemorrhage (19). Mice lacking an individual integrin, αvβ3, αvβ5, or αvβ6, are all viable and fertile and do not develop hemorrhage in the brain (22, 23, 24). Additionally, we show here that embryos genetically null for both the β3 and β5 integrin genes proceed through embryogenesis without developing cerebral hemorrhage (Fig. 9).

Rather, the abnormal vasculature in αv-null embryos is apparently due to the loss of integrin αvβ8. αvβ8 is strongly expressed in the adult central nervous system (29) and on cultured embryonic and postnatal central nervous system glia and is required for proper glial cell migration in vitro (28). While this paper was in revision, ablation of the gene encoding the β8 integrin subunit was reported to lead to cerebral hemorrhage and early postnatal lethality (38). The phenotype of the β8-null mice is strikingly similar in all major aspects to that of the αv knockouts reported here and elsewhere (3).

Vitronectin is the primary extracellular matrix ligand for αvβ8 and is expressed in the basement membrane of embryonic cerebral microvessels (35). It is quite possible that loss of αvβ8 could render the brain parenchymal cells incapable of normal adherence to the perivascular sheath. Likewise, central nervous system parenchyma-specific intracellular signaling pathways regulated by αvβ8 adhesion could play roles in maintaining normal cerebral vessel-parenchymal cell associations. It is well established that maintenance of proper microvessel function requires secreted growth factors as well as cell-cell contacts between endothelial cells and pericytes (6). Thus, it is quite likely that similar events occur between the brain parenchymal cells and the associated microvascular sheath (composed of the endothelial cell and pericyte). Whether this regulation occurs directly between the endothelial cell and parenchymal cells or is relayed via the pericytes remains to be determined.

In conclusion, our results show that cells of the central nervous system brain parenchyma are involved in regulating cerebral blood vessel integrity via αv integrins, specifically αvβ8. The study of cultured brain parenchymal cells (radial glia and neuroblasts) as well as conditional deletion of the αv and/or β8 gene in a cell-specific context will certainly prove useful in better understanding the mechanisms underlying these events.

ACKNOWLEDGMENTS

We thank Dean Sheppard for providing the β5-null mice, Denise Crowley for expert histology technical assistance, Patricia Fox and Kathryn Pyne for ultrastructural technical assistance, and Daniela Taverna, Herbert Haack, and Charlie Whittaker for critical reading of the manuscript.

This work was supported in part by a grant from the Swedish Cancer Foundation to K.R., Deutsche Forschungsgemeinschaft-SPP 1069 to B.L.B., grants from the National Heart, Lung, and Blood Institute (HL66105-02 and HL41484-08) and Howard Hughes Medical Institute to R.O.H., and grants from the Allergy and Immunology Institute of the NIH (AI3372 and AI44066) to A.M.D. J.H.M. is an Associate and R.O.H. is an Investigator of the Howard Hughes Medical Institute.

REFERENCES

1. **Alvarez-Buylla, A., J. M. Garcia-Verdugo, and A. D. Tramontin.** 2001. A unified hypothesis on the lineage of neural stem cells. Nat. Rev. Neurosci. **2:**287–293.
2. **Anton, E. S., J. A. Kreidberg, and P. Rakic.** 1999. Distinct functions of α3 and αv integrin receptors in neuronal migration and laminar organization of the cerebral cortex. Neuron **22:**277–289.
3. **Bader, B. L., H. Rayburn, D. Crowley, and R. O. Hynes.** 1998. Extensive vasculogenesis, angiogenesis, and organogenesis precede lethality in mice lacking all alpha v integrins. Cell **95:**507–519.
4. **Balabanov, R., and P. Dore-Duffy.** 1998. Role of the central nervous system microvascular pericyte in the blood-brain barrier. J. Neurosci. Res. **53:**637–644.
5. **Bass, T., G. Singer, J. Slusser, and F. J. Liuzzi.** 1992. Radial glial interaction with cerebral germinal matrix capillaries in the fetal baboon. Exp. Neurol. **118:**126–132.
6. **Beck, L., Jr., and P. A. D'Amore.** 1997. Vascular development: cellular and molecular regulation. FASEB J. **11:**365–373.
7. **Brooks, P. C., R. A. Clark, and D. A. Cheresh.** 1994. Requirement of vascular integrin αvβ3 for angiogenesis. Science **264:**569–571.
8. **Brooks, P. C., A. M. Montgomery, M. Rosenfeld, R. A. Reisfeld, T. Hu, G. Klier, and D. A. Cheresh.** 1994. Integrin αvβ3 antagonists promote tumor regression by inducing apoptosis of angiogenic blood vessels. Cell **79:**1157–1164.
9. **Carmeliet, P., V. Ferreira, G. Breier, S. Pollefeyt, L. Kieckens, M. Gertsenstein, M. Fahrig, A. Vandenhoeck, K. Harpal, C. Eberhardt, C. Declercq, J. Pawling, L. Moons, D. Collen, W. Risau, and A. Nagy.** 1996. Abnormal blood vessel development and lethality in embryos lacking a single VEGF allele. Nature **380:**435–439.
10. **Carmeliet, P., M. G. Lampugnani, L. Moons, F. Breviario, V. Compernolle, F. Bono, G. Balconi, R. Spagnuolo, B. Oostuyse, M. Dewerchin, A. Zanetti, A. Angellilo, V. Mattot, D. Nuyens, E. Lutgens, F. Clotman, M.C. de Ruiter, A. Gittenberger-de Groot, R. Poelmann, F. Lupu, J. M. Herbert, D. Collen, and E. Dejana.** 1999. Targeted deficiency or cytosolic truncation of the VE-cadherin gene in mice impairs VEGF-mediated endothelial survival and angiogenesis. Cell **98:**147–157.
11. **Chanas-Sacre, G., B. Rogister, G. Moonen, and P. Leprince.** 2000. Radial glia phenotype: origin, regulation, and transdifferentiation. J. Neurosci. Res. **61:**357–363.
12. **Drake, C. J., D. A. Cheresh, and C. D. Little.** 1995. An antagonist of integrin αvβ3 prevents maturation of blood vessels during embryonic neovascularization. J. Cell Sci. **108:**2655–2661.
13. **Dvorak, A. M.** 1987. Procedural guide to specimen handling for the ultrastructural pathology service laboratory. J. Electron Microsc. Techniques **6:**255–301.
14. **Fassler, R., and M. Meyer.** 1995. Consequences of lack of β1 integrin gene expression in mice. Genes Dev. **9:**1896–1908.
15. **Ferrara, N., K. Carver-Moore, H. Chen, M. Dowd, L. Lu, K.S. O'Shea, L. Powell-Braxton, K. J. Hillan, and M. W. Moore.** 1996. Heterozygous embryonic lethality induced by targeted inactivation of the VEGF gene. Nature **380:**439–442.
16. **Friedlander, M., P. C. Brooks, R. W. Shaffer, C. M. Kincaid, J. A. Varner, and D. A. Cheresh.** 1995. Definition of two angiogenic pathways by distinct αv integrins. Science **270:**1500–1502.
17. **Friedlander, M., C. L. Theesfeld, M. Sugita, M. Fruttiger, M. A. Thomas, S. Chang, and D. A. Cheresh.** 1996. Involvement of integrins αvβ3 and αvβ5 in ocular neovascular diseases. Proc. Natl. Acad. Sci. USA **93:**9764–9769.
18. **Gerhardt, H., H. Wolburg, and C. Redies.** 2000. N-Cadherin mediates pericytic-endothelial interaction during brain angiogenesis in the chicken. Dev. Dyn. **218:**472–479.
19. **Graus-Porta, D., S. Blaess, M. Senften, A. Littlewood-Evans, C. Damsky, Z. Huang, P. Orban, R. Klein, J. C. Schittny, and U. Muller.** 2001. β1-Class integrins regulate the development of laminae and folia in the cerebral and cerebellar cortex. Neuron **31:**367–379.
20. **Hellstrom, M., M. Kaln, P. Lindahl, A. Abramsson, and C. Betsholtz.** 1999. Role of PDGF-B and platelet-derived growth factor receptor beta in recruitment of vascular smooth muscle cells and pericytes during embryonic blood vessel formation in the mouse. Development **126:**3047–3055.
21. **Hellstrom, M., H. Gerhardt, M. Kalen, U. Eriksson, H. Wolburg, and C. Betsholtz.** 2001. Lack of pericytes leads to endothelial hyperplasia and abnormal vascular morphogenesis. J. Cell Biol. **153**:543–553.
22. **Hodivala-Dilke, K. M., K. P. McHugh, D. A. Tsakiris, H. Rayburn, D. Crowley, M. Ullman-Cullere, F. P. Ross, B. S. Coller, S. Teitelbaum, and R. O. Hynes.** 1999. β3-Integrin-deficient mice are a model for Glanzmann thrombasthenia showing placental defects and reduced survival. J. Clin. Investig. **103:**229–238.
23. **Huang, X., M. Griffiths, J. Wu, R. V. Farese, Jr., and D. Sheppard.** 2000. Normal development, wound healing, and adenovirus susceptibility in β5-deficient mice. Mol. Cell. Biol. **20:**755–759.
24. **Huang, X., J. Wu, W. Zhu, R. Pytela, and D. Sheppard.** 1998. Expression of the human integrin beta6 subunit in alveolar type II cells and bronchiolar epithelial cells reverses lung inflammation in β6 knockout mice. Am. J. Respir. Cell. Mol. Biol. **19:**636–642.
25. **Janzer, R. C., and M. C. Raff.** 1987. Astrocytes induce blood-brain barrier properties in endothelial cells. Nature **325:**253–257.
26. **Marin-Padilla, M.** 1985. Early vascularization of the embryonic cerebral cortex: Golgi and electron microscopic studies. J. Comp. Neurol. **241:**237–249.
27. **Milner, R., X. Huang, J. Wu, S. Nishimura, R. Pytela, D. Sheppard, and C. ffrench-Constant.** 1999. Distinct roles for astrocyte αvβ5 and αvβ8 integrins in adhesion and migration. J. Cell Sci. **112:**4271–4279.
28. **Milner, R., J. B. Relvas, J. Fawcett, and C. ffrench-Constant.** 2001. Developmental regulation of αv integrins produces functional changes in astrocyte behavior. Mol. Cell. Neurosci. **18:**108–118.
29. **Nishimura, S. L., K. P. Boylen, S. Einheber, T. A. Milner, D. M. Ramos, and R. Pytela.** 1998. Synaptic and glial localization of the integrin αvβ8 in mouse and rat brain. Brain Res. **791:**271–282.
30. **Noctor, S. C., A. C. Flint, T. A. Weissman, R. S. Dammerman, and A. R. Kriegstein.** 2001. Neurons derived from radial glial cells establish radial units in neocortex. Nature **409:**714–720.

31. **Ozerdem, U., K. A. Grako, K. Dahlin-Huppe, E. Monosov, and W. B. Stallcup.** 2001. NG2 proteoglycan is expressed exclusively by mural cells during vascular morphogenesis. Dev. Dyn. **222:**218–227.
32. **Peters, J. H., G. E. Chen, and R. O. Hynes.** 1996. Fibronectin isoform distribution in the mouse. II. Differential distribution of the alternatively spliced EIIIB, EIIIA, and V segments in the adult mouse. Cell Adhes. Commun. **4:**127–148.
33. **Risau, W., and H. Wolburg.** 1990. Development of the blood-brain barrier. Trends Neurosci. **13:**174–178.
34. **Rubin, L. L., and J. M. Staddon.** 1999. The cell biology of the blood-brain barrier. Annu. Rev. Neurosci. **22:**11–28.
35. **Seiffert, D., M. L. Iruela-Arispe, E. H. Sage, and D. J. Loskutoff.** 1995. Distribution of vitronectin mRNA during murine development. Dev. Dyn. **203:**71–79.
36. **Suri, C., P. F. Jones, S. Patan, S. Bartunkova, P. C. Maisonpierre, S. Davis, T. N. Sato, and G. Yancopoulos.** 1996. Requisite role of angiopoietin-1, a ligand for the Tie2 receptor, during embryogenesis. Cell **87:**1171–1180.
37. **Tidhar, A., M. Reichenstein, D. Cohen, A. Faerman, N. G. Copeland, D. J. Gilbert, N. A. Jenkins, and M. Shani.** 2001. A novel transgenic marker for migrating limb muscle precursors and for vascular smooth muscle cells. Dev. Dyn. **220:**60–73.
38. **Zhu, J., K. Motejlek, D. Wang, A. Schmidt, and L. F. Reichardt.** 2002. β8 integrins are required for vascular morphogenesis in mouse embryos. Development **129:**2891–2903.